

Plateau-Rayleigh instability in a torus: formation and breakup of a polymer ring

Joshua D. McGraw,^a Jianfeng Li,^{ab} David L. Tran,^a An-Chang Shi^a and Kari Dalnoki-Veress^{*a}

Received 21st September 2009, Accepted 11th December 2009

First published as an Advance Article on the web 29th January 2010

DOI: 10.1039/b919630g

A liquid jet can break up into a stream of droplets as a result of the Plateau-Rayleigh instability. The droplet formation decreases the jet's surface area and hence its free energy. Here we present the results of experiments in an unconventional geometry where this instability can be observed: a toroidal section. We discuss the formation of these polystyrene toroids with nanometer length scales. The constraints imposed by this geometry affect its observed instability in comparison to a simple linear jet. Specifically, we show that the additional curvature imposed by the torus can have a significant impact on the energy minimization route.

Introduction

The Plateau-Rayleigh (P-R) instability is responsible for the breakup that occurs when a long cylindrical fluid body with a free surface is allowed to evolve. A familiar example of this instability can be seen when water flows from a faucet and falls under the influence of gravity;¹ a less familiar example has recently been observed in a falling granular stream.² Near the point of exit a stream is cylindrical. Further away the system lowers its free energy *via* a sinusoidal undulation of the surface which eventually grows to the point of pinching off into a series of droplets. Much effort has been devoted to understanding the breakup of fluid streams in the last century and a half, and a comprehensive review can be found elsewhere.¹ However, comparatively little has even been observed of this effect in geometries other than long straight cylinders.

Recently, the creation and observed breakup of liquid toroids was reported in elegant experiments by Pairam and Fernández-Neives.³ These authors used a novel method of producing macroscopic water toroids suspended in viscous liquids with precise control of the overall ring radius, r , and the radius of the cylinder, a (see schematic in Fig. 1(a)). Pairam and Fernández-Neives carried out a systematic study of the breakup of individual toroids and the dependence on the aspect ratio, r/a . The liquid toroids eventually break up into a number of spherical droplets as a means of decreasing its surface energy. However, for a torus, the wavelength of the instability must be commensurate with the tube's circumference. This additional constraint imposed by the geometry of a torus undergoing the P-R instability was observed by Pairam and Fernández-Neives.³

Owing to the fact that a liquid torus is unstable, the difficulty in preparing them is noteworthy. Pairam and Fernández-Neives prepared toroids with a water filled needle immersed in a rotating bath of an immiscible viscous liquid.³ Recently it was shown that

a torus can form as a droplet falls in air as a result of the interactions between the droplet and its surrounding atmosphere. Interestingly, the breakup of that torus has a role to play in determining the distribution of drop sizes during rainfall.⁴ For these formation mechanisms, the short time interval between formation and breakup is the limiting factor in making observations on a torus. As we will show, an advantage of polymeric systems is that it is possible to prepare toroids in the glassy state which can then transition into the melt state in an easily controllable manner. The ability to transition from the melt to the glassy state enables observation of the toroids at any stage of the breakup process.

Here we report a method of preparing solid polystyrene (PS) toroids with micron sized ring radii and nanoscale cylinder radii. The method produces a collection of solid toroidal sections on a substrate with various aspect ratios. A typical example of such a toroidal section, before and after the P-R instability, is shown in the atomic force microscopy (AFM) topography images of

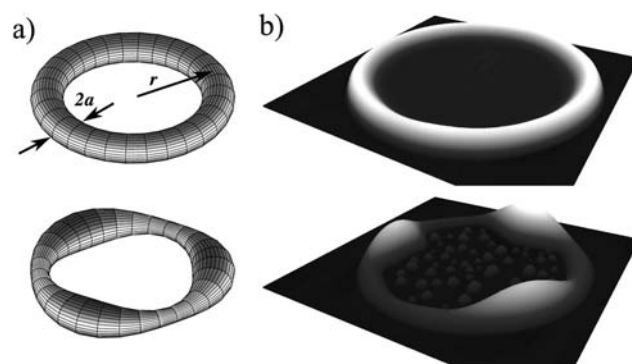


Fig. 1 (a) Schematic of a torus where r is the overall radius of the ring and a is the radius of the cylinder. Also shown is an intermediate stage of a liquid torus undergoing surface undulations due to the Plateau-Rayleigh instability. (b) AFM topography images analogous to the schematics shown in (a). For this example the polystyrene ring has a diameter of $28.5\ \mu\text{m}$ and toroidal section has a height of $135\ \text{nm}$. Note that the small droplets inside the ring are the result of a very thin film that has dewetted.

^aDepartment of Physics & Astronomy and the Brockhouse Institute for Materials Research, McMaster University, Hamilton, Canada. E-mail: dalnoki@mcmaster.ca

^bDepartment of Macromolecular Science, Fudan University, Shanghai, 200433, China

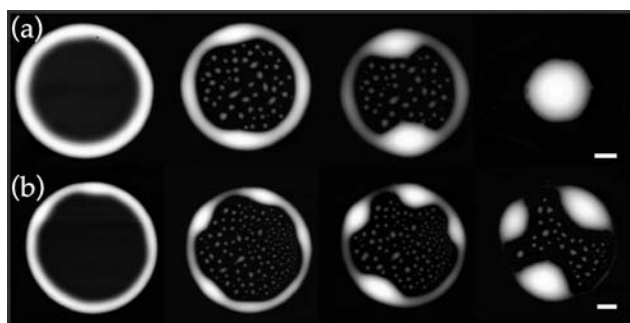


Fig. 2 Evolution of two PS toroidal sections as observed with AFM. The images were obtained by quenching the sample at various stages allowing the imaging to take place in the glassy state. The scale bars are $5\ \mu\text{m}$ wide; height scales are both approximately $160\ \text{nm}$ in (a) and (b); in the fourth column the height scales are $\sim 400\ \text{nm}$ for (a) and $\sim 230\ \text{nm}$ for (b).

Fig. 1(b). PS toroids can easily be made to undergo a transition from the solid to melt state and the approach to equilibrium can be recorded while the system is viewed under an optical microscope. The approach to equilibrium can be halted and any intermediate state can then be observed using AFM (see images in Fig. 2). As was the case for the macroscopic toroids of Páram and Fernández-Neives,³ we find that the evolution of the nano-scale toroidal sections are influenced by the geometric constraints.

Experimental

To create the glassy polystyrene toroids, we place a bath of methanol onto a $1 \times 1\ \text{mm}^2$ Si substrate (University Wafer). The

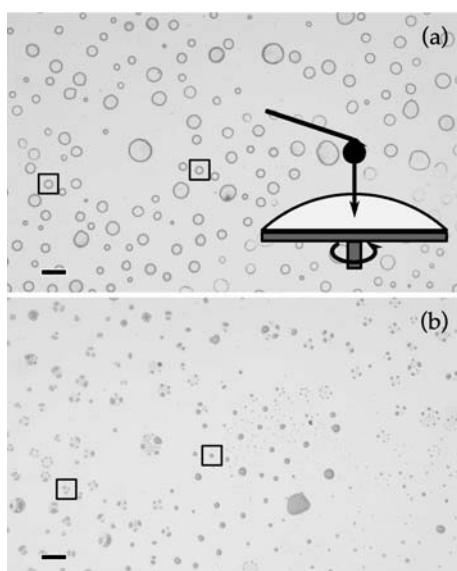


Fig. 3 The schematic illustrates the sample preparation: a small droplet of PS dissolved in toluene falls from a small syringe needle onto a substrate covered with methanol. Spincoating is immediately initiated and most of the three component solution is ejected from the substrate. After spincoating is completed, toroidal sections of PS are found on the substrate as shown in the optical microscopy image (a). The image in (b) is obtained after annealing the sample in a toluene saturated atmosphere for time periods of order two hours or less. The boxes indicate the two rings shown in the first and fourth columns of Fig. 2. The scale bars are $100\ \mu\text{m}$.

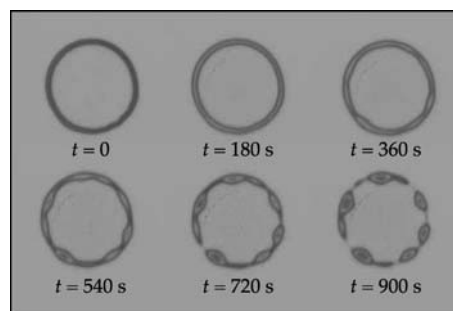


Fig. 4 The observed evolution of a PS torus in an atmosphere saturated with toluene. N , the number of wavelengths observed was counted at the onset of the P-R instability similar to the image shown at $t = 540\ \text{s}$.

substrate is on a stationary spincoater over which a syringe filled with PS dissolved in toluene is placed (see schematic in Fig. 3(a)). The PS (Polymer Source Inc.) has molecular weight $M_w = 221\ \text{kg/mol}$ and polydispersity index of 1.03. A small drop of the solution is allowed to fall into the methanol bath and spincoating ($\sim 4000\ \text{rpm}$) is immediately initiated as indicated schematically in Fig. 3(a). Toluene is a good solvent for PS and is miscible with methanol. Methanol is a non-solvent for PS. The spincoating process ejects most of the fluid and upon completion leaves behind a collection of toroidal sections with distributions of radii r , and cylinder widths w . Here we assume that the contact angle with the substrate is constant for all toroids and hence the cylinder radius $a \propto w$. Concentrations of 0.1 to 1 wt% PS have been observed to produce toroidal sections. A typical image of the resulting sample is shown in Fig. 3(a).

Once toroidal sections have been prepared, the samples are placed in a toluene saturated atmosphere.^{5,6} Since toluene is a good solvent for PS, the toroidal sections absorb toluene which causes them to transition from the glassy to the melt state. The geometry in which the toroids are prepared is unstable and the rings eventually dewet to form droplets which minimize the free energy of the system. Images are taken with a CCD camera at periodic intervals using optical microscopy. The end result of this process is shown in Fig. 3(b). In Fig. 4 a series of optical microscopy images illustrating the evolution of the instability for a single torus is shown. For several samples, the dewetting process has been paused at various stages by removing the toluene atmosphere and quenching into the glassy state. Once the evolution was halted, the samples were imaged with AFM (Veeco Caliber). The evolution could be commenced simply by re-immersing the sample in the toluene saturated atmosphere. Results of this process are shown in Fig. 2.

Results and discussion

Formation of toroids

There has been significant interest in the formation of ‘rings’ especially as a result of work done by Deegan and coworkers which was inspired by the formation of coffee stains.⁷ It was shown by these authors that the formation of a ring resulting from a drying drop of a colloidal suspension was in part the result of greater evaporation near the contact line. The enhancement of evaporation causes an outward flow

towards the edge of the droplet and subsequent ring formation due to aggregation of the colloids at the contact line. Similar results are obtained for the drying of a droplet of polymer solution.^{8–10} The concentration gradients in a drying droplet were recently visualized directly using fluorescence microscopy by Kajiya and coworkers for a polymer solution drying in air.⁸ In these systems large polymeric rings ($r \sim$ millimeters) were formed similar to the ones described in the study presented here. Poulard and Damman⁹ investigated the importance of the substrate properties and the various interfacial tensions to the formation of a ring at the edge of a drying droplet. In the system discussed here there is no droplet that is drying in air, though we propose a mechanism that borrows from what has been learned from such systems.^{7–9}

Although we cannot directly observe the formation of polymer toroids, we propose the following mechanism for their formation. As the PS and toluene solution enters the methanol reservoir, spin coating is immediately initiated. The spinning substrate accelerates and shears the three component mixture and produces tiny droplets of the PS solution in methanol, a fraction of which land on the Si substrate and make some contact angle with the surface. This initial step is highly complex and we cannot experimentally follow this process directly because of the rapid speed with which this occurs (fraction of a second). The size distribution of the tori, and even the presence of tori, is sensitive to the timing and spin speed. We find that the spinning must be initiated immediately as the droplet of PS and toluene solution hits the methanol. If the process takes too long, the PS precipitation has proceeded too far and a fine dispersion of PS particles is found on the substrate rather than tori. With careful timing of the process the results are reproducible with tori distributed randomly on the substrate and ring radii ranging from several micrometers to a few tens of micrometers. The second step proceeds once small droplets of PS in toluene surrounded by methanol contact the substrate. We suggest that the process by which the rings form is analogous to the outward flow responsible for ring formation in drying droplets of polymer solutions^{8–11} or colloidal dispersions.⁷ In our case the PS precipitates out of the toluene solutions as soon as the miscible methanol and toluene mix at the interface of the droplet. As in the case of a colloidal dispersion, the PS precipitate is driven towards the contact line both because of pinning at the substrate and the higher flux of toluene near the contact line.^{7–11} As shown by Poulard and Damman⁹ the Marangoni effect can drive flow at the interface especially for the case of droplets drying in air. Because the interface between the PS solution droplet and the methanol vanishes rapidly due to the miscibility of the two solvents, the flow driven by the osmotic pressure is dominant.⁷ We note that the enhanced flux at the contact line is the result of the boundary imposed by the substrate causing an anisotropy in the diffusion of toluene and methanol. The final result is a toroidal ring of polymer on a substrate with a very thin film of polymer inside the ring (see Fig. 1(b)).

In order to further substantiate the proposed mechanism for the formation of the toroids, we turn to simulations of the phase separation of a ternary mixture composed of methanol, toluene and PS. Methanol is known to be miscible with toluene but immiscible with PS, whereas toluene is miscible with PS. The

free energy of the ternary mixture can be described by the Flory-Huggins¹² theory supplemented with the de Gennes¹³ gradient contribution,

$$\Delta f = \phi_m \ln \phi_m + \phi_t \ln \phi_t + \frac{\phi_p \ln \phi_p}{N_p} + \chi_{m,p} \phi_m \phi_p + \chi_{m,t} \phi_m \phi_t + \chi_{t,p} \phi_t \phi_p + \sum_{i=m,t,p} \bar{\kappa}_{ii} (\nabla \phi_i)^2 \quad (1)$$

where ϕ_i is the local volume fraction of component i and is a function of position; $\chi_{i,j}$ is the Flory-Huggins interaction parameter between components i and j ; the subscripts m , t and p represent methanol, toluene and polystyrene respectively; and N_p is the degree of polymerization of the PS. The gradient energy coefficients, $\bar{\kappa}_{ii}$, are assumed to be constant for a system with constant overall concentrations, ϕ_i . For a given initial polymer concentration, which is in general not at equilibrium, the dynamics of the system can be described by the time-dependent Ginzburg-Landau (TDGL) theory.¹⁴

In our simulation boxes (ranging in size from $100 \times 100 \times 25$ to $400 \times 400 \times 100$), we start with a spherical cap that has a contact angle $\theta = \pi/6$. The cap is filled by a homogeneous ‘PS’ and ‘toluene’ mixture ($\phi_p = 0.0025$, $\phi_t = 1 - \phi_p$ and $\phi_m = 0$) with $\chi_{t,p} = 0.0$ and $N_p = 2000$. Outside the spherical cap, the box is filled with ‘methanol’ ($\phi_p = \phi_t = 0$ and $\phi_m = 1$). The interaction parameters are specified by $\chi_{m,t} = 0$ and $\chi_{m,p} = 8$.¹⁵ These parameters reflect the fact that, toluene and methanol are miscible, PS is miscible with toluene, and PS is immiscible with methanol. The boundary conditions are chosen to be reflective at the substrate. All the other boundaries are such that when a toluene molecule comes in contact with the wall it is replaced by methanol in order to simulate the infinite methanol bath. With this initial condition, the equations of motion defined using eqn (1) have been evolved in time. Fig. 5 shows the evolution of one such simulation, clearly demonstrating that the phase separation coupled with solvent mixing can produce polymer toroids. The simulation does not include the evaporation of the two solvents from the system and the eventual freezing of the polymer. We assume that during the final evaporation stage, the structure collapses onto the substrate and freezes leaving the tori resembling the integrated PS concentration shown in 5(b).

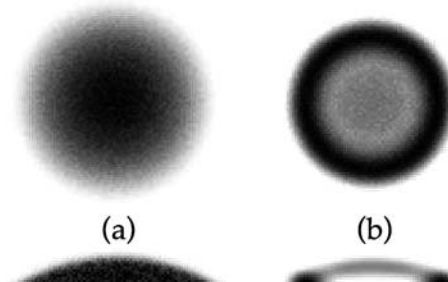


Fig. 5 The formation of a PS torus for a simulation box with dimensions $100 \times 100 \times 25$. The initial, homogeneous state of the spherical cap is shown in (a). Some time later a ring is formed, as shown in (b). The gray level is proportional to the integrated PS concentration from the top to the bottom of the simulation box (top row), or the radially integrated PS concentration (bottom row). White indicates no PS.

Instability

Having discussed the formation of the toroids, we now turn to the instability which occurs when a torus is free to flow (for a typical example see Fig. 4). When a toroidal section is exposed to a toluene saturated atmosphere, the PS, which is in the glassy state at room temperature in air, is plasticized by the toluene and is in the melt state. The PS becomes mobile and flow proceeds in the direction that decreases free energy the fastest. The P-R instability drives the toroidal section to break up into droplets. The number of droplets formed is determined by the wavelength of the instability. Using either linear stability analysis or Rayleigh's work principle, it can be shown that the 'most dangerous' (fastest growing) wavelength is proportional to the cylinder radius, a . It is this wavelength that we associate with the onset of the instability observed in our experiments.^{1,16} From an image as shown in Fig. 4 at $t = 540$ s it is possible to measure the number of wavelengths, N , that fit in the toroidal section. Since the width, w , of the toroidal section is proportional to the radius of the cylinder, a , we can write $N \sim r/w$.

As shown in Fig. 3, the method of producing the solid polymer toroids presented here yields sections with a variety of values of overall ring radii, r , and section widths, w . In Fig. 6(a), the line intensity profile of a toroidal section as observed in an optical microscopy image is shown. From line profiles such as these, one can measure values of r and w . In Fig. 6(b) a plot of the number of wavelengths that fit on the toroids, N , as a function of the measured ratio r/w is shown. The value of r/w is measured just prior to the observation of the P-R instability. As expected from the simple linear stability analysis,^{1,16} N is linear in r/w .

The preceding argument has assumed that the curvature of the overall ring radius, r , of the toroidal sections does not contribute to their evolution in the liquid state. However, a torus has two routes by which the free energy can be reduced: 1) the P-R instability, as discussed above; and 2) by evolving towards a ring with a smaller radius, r , while the width of the ring, w , increases to maintain a constant volume. For the latter route, letting $r_\varepsilon = r - \varepsilon$ and with volume conservation, it is easy to show that the ratio of the areas of the torus before and after a small change in r is, to first order in ε ,

$$\frac{\mathcal{A}_\varepsilon}{\mathcal{A}} = 1 - \frac{\varepsilon}{2r} \quad (2)$$

Note that this ratio is less than unity for all $\varepsilon > 0$; therefore, a torus can reduce its surface area and hence its free energy by

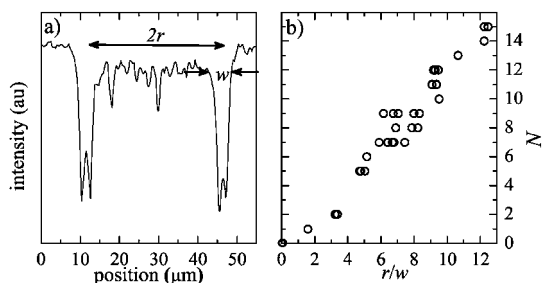


Fig. 6 (a) A line profile of a ring similar to the one shown in Fig. 4 at $t = 180$ s. From this line profile, r , and w , are easily obtained. (b) A plot of the number of wavelengths around a torus as a function of the ratio of the overall radius to the section width, r/w at similar stages of development. N is linear in r/w as expected from the P-R instability.

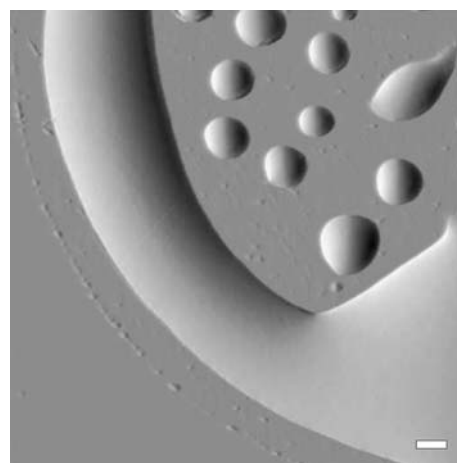


Fig. 7 AFM error signal of the ring shown in the third column of Fig. 2(a). About $1 \mu\text{m}$ from the three phase contact line of the main ring, a thin concentric halo is clearly visible which suggests that r is decreasing with time. The scale bar is $1 \mu\text{m}$.

decreasing r . Because volume is conserved, this decrease in r is accompanied by an increase in the width, w , of the torus on the substrate. The balance between these two mechanisms depends on which timescale dominates. If the curvature $1/r$ becomes comparable to the curvature that dominates the timescale of the P-R instability, $1/a$ (or $1/w$), then we would expect the ring radius to shrink during the experiment.

In Fig. 7, we show a detail of the AFM error signal (roughly, the derivative of the topography) of the ring shown in the third column of Fig. 2(a). Around the outer three phase contact line of the ring, there is a clearly visible remnant of the ring in its initial state. As expected in cases where the time scale of the P-R instability does not dominate, this example shows that the torus decreases its radius, r . Because of the observation that the ring radius can decrease prior to the onset of the P-R instability (Fig. 7) the values of r/w in Fig. 6 are obtained just prior to the onset of the P-R instability.

The effect of decreasing the free energy by reducing the ring radius is to decrease the ratio r/w as a function of time until the P-R instability dominates. In order to validate this second mechanism we followed the time evolution of the outer diameter of a ring using AFM during the onset of the instability. In Fig. 8

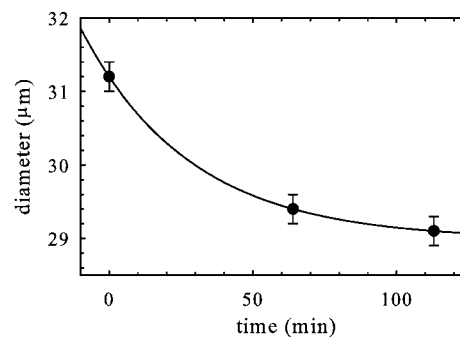


Fig. 8 A plot of the outside diameter of a torus as a function of annealing time during the evolution of the instability (solid line to guide the eye). The data in this plot corresponds to the first three AFM images shown in Fig. 2(a).

the shrinking of the ring with time is clearly visible indicating that the two mechanisms, the P-R instability and decreasing ring radius, compete with the balance set by the curvatures given by $1/a$ and $1/r$ respectively.

Taking into account both the cylinder curvature which drives the P-R instability, $1/a$, and the curvature, $1/r$, which drives the ring radius to decrease, a complex interplay between these two mechanisms emerges. The maximally unstable wavelength for the P-R instability may not be commensurate with the torus, thus the free energy is reduced *via* a decrease in the ring radius. Eventually the torus becomes commensurate with a P-R wavelength which dominates the reduction of the surface area. While for simplicity we have discussed these mechanisms as two subsequent steps, in fact both mechanisms are competing with the P-R instability dominating in the last stage.

Conclusion

We have presented a novel method by which a collection of solid PS toroidal sections with micro- and nano-scale dimensions can be prepared on a substrate. The method requires a solution of the polymer in a good solvent to be dropped into a miscible bath of poor solvent for the polymer. Here the ternary system used was PS, toluene, and methanol. We provide evidence for a formation mechanism which is similar to the way in which coffee stains form or polymer solution droplets dry.⁷⁻¹¹ Experiments have been carried out in which the polymer toroids were allowed to evolve in the melt state. As would be the case for a linear jet, the P-R instability is responsible for their breakup. In contrast to the straight liquid jet we have shown that the additional curvature of the torus provides a second mechanism by which these structures can minimize their free energy – the ring radius can decrease. In

order for the P-R instability to grow the wavelengths of the instability must be commensurate with the circumference of each torus. In the cases where the fastest growing P-R wavelength for a torus does not drive the instability too quickly, the competing mechanism which acts to shrink the ring radius can be observed.

Acknowledgements

Financial support from NSERC of Canada is gratefully acknowledged.

References

- 1 J. Eggers, *Rev. Mod. Phys.*, 1997, **69**, 865.
- 2 J. Royer, D. Evans, L. Oyarte, Q. Guo, E. Kapit, M. Möbius, S. Waitukaitis and H. Jaeger, *Nature*, 2009, **459**, 1110.
- 3 E. Pairam and A. Fernández-Nieves, *Phys. Rev. Lett.*, 2009, **102**, 234501.
- 4 E. Villermaux and B. Bossa, *Nat. Phys.*, 2009, **5**, 697.
- 5 L. Xu, T. Shi, P. Dutta and L. An, *J. Chem. Phys.*, 2007, **127**, 144704.
- 6 S. Lee, P. Yoo, S. Kwon and H. Lee, *J. Chem. Phys.*, 2004, **121**, 4346.
- 7 R. Deegan, O. Bakajin, T. Dupont, G. Huber, S. Nagel and T. Witten, *Nature*, 1997, **389**, 827.
- 8 T. Kajiya, D. Kaneko and M. Doi, *Langmuir*, 2008, **24**, 12369.
- 9 C. Poulard and P. Damman, *Europhys. Lett.*, 2007, **80**, 64001.
- 10 H. Hu and R. G. Larson, *Langmuir*, 2005, **21**, 3963.
- 11 F.-I. Li, P. H. Leo and J. A. Barnard, *J. Phys. Chem. B*, 2008, **112**, 16497.
- 12 M. Rubinstein and R. Colby, *Polymer Physics*, Oxford University Press, 2003.
- 13 P. de Gennes, *J. Chem. Phys.*, 1980, **72**, 4756.
- 14 C. Huang, M. de La Cruz and B. Swift, *Macromolecules*, 1995, **28**, 7996.
- 15 N. Schulz and B. Wolf, *Polymer Handbook*, John Wiley & Sons, Inc., 1999, vol. 4, (ch. VII), p. 247.
- 16 L. E. Johns and R. Narayanan, *Interfacial Instability*, Springer, 2002.